A Nonlinear Electrostatic Potential Change in the T-System of Skeletal Muscle Detected Under Passive Recording Conditions Using Potentiometric Dyes

JUDITH A. HEINY and DE-SHIEN JONG

From the Department of Physiology and Biophysics, University of Cincinnati, College of Medicine, Cincinnati, Ohio 45267-0576; and the Department of Physics, University of Cincinnati, Cincinnati, Ohio 45267-0011

ABSTRACT Voltage-sensing dyes were used to examine the electrical behavior of the T-system under passive recording conditions similar to those commonly used to detect charge movement. These conditions are designed to eliminate all ionic currents and render the T-system potential linear with respect to the command potential applied at the surface membrane. However, we found an unexpected nonlinearity in the relationship between the dye signal from the T-system and the applied clamp potential. An additional voltage- and time-dependent optical signal appears over the same depolarizing range of potentials where charge movement and mechanical activation occur. This nonlinearity is not associated with unblocked ionic currents and cannot be attributed to lack of voltage clamp control of the T-system, which appears to be good under these conditions. We propose that a local electrostatic potential change occurs in the T-system upon depolarization. An electrostatic potential would not be expected to extend beyond molecular distances of the membrane and therefore would be sensed by a charged dye in the membrane but not by the voltage clamp, which responds solely to the potential of the bulk solution. Results obtained with different dyes suggest that the location of the phenomena giving rise to the extra absorbance change is either intramembrane or at the inner surface of the T-system membrane.

INTRODUCTION

Charge movement currents are normally recorded in response to voltage-clamp pulses applied across the surface membrane, from muscle fibers perfused with solutions designed to eliminate all ionic currents (Schneider and Chandler, 1973; Chandler et al., 1976*a*). However, the molecular species that give rise to charge

Address reprint requests to Dr. Judith A. Heiny, Department of Physiology and Biophysics, University of Cincinnati College of Medicine, Mail Location 576, 231 Bethesda Avenue, Cincinnati, OH 45267-0576.

Dr. Jong's present address is Department of Cellular and Molecular Physiology, Yale University School of Medicine, New Haven, CT 06510.

J. GEN. PHYSIOL. © The Rockefeller University Press · 0022-1295/90/01/0147/29 $2.00
Volume 95 January 1990 147–175

movement reside mainly in the T-system membranes and respond directly to the T-system transmembrane potential. Because electrically the T-system represents a distributed cable in contact with the surface membrane, it is expected that a finite amount of time will be required to charge the T-system to a new potential, and that there will be some decrement of potential along the fiber radius in the steady-state (Falk, 1968; Adrian et al., 1969). Under typical charge movement recording conditions it is generally assumed that the tubular membrane resistance is sufficiently large that this radial decrement will be small and that, after a charging time of a few milliseconds, the T-system will come to a uniform, constant potential equal to that imposed at the surface membrane. A corrollary assumption is that the steady-state T-system voltage will be linearly related to the applied clamp potential over the entire voltage range, i.e., at voltages where charge movement is elicited as well as at voltages used for subtraction of the linear fiber capacitance. However, these assumptions have never been directly tested because the dimensions of the tubules render them physically inaccessible to conventional microelectrodes.

In recent years, it has become possible to follow T-system potential changes optically using voltage-sensing dyes, and to separate the optical signals originating in the T-system from those contributed by the surface membrane (Nakajima and Gilai, 1980; Vergara and Bezanilla, 1981; Heiny and Vergara, 1982, 1984). The purpose of the present experiments was to examine the electrical response of the T-system under charge movement recording conditions using potentiometric dyes.

Preliminary reports of this work have appeared (Jong and Heiny, 1988, 1989; Heiny and Jong, 1989).

METHODS

Experimental Preparation and Protocols

The experiments were performed using single cut skeletal muscle fibers from the semitendinosus muscle of *Rana catesbiana*. The fibers were voltage clamped using a vaseline-gap method. The voltage-clamp chamber and electronics were based on that of Hille and Campbell (1976), and adapted for optical recording as described previously (Heiny and Vergara, 1984).

Briefly, single fiber segments of 2–3 cm length and 100–160 μm diameter were dissected and stimulated extracellularly to verify that an all-or-nothing fast twitch could be elicited. The segments were transferred to a small plastic dish, stretched slightly, then perfused with a high potassium, calcium-free relaxing solution (Table I) which caused a transient contraction followed by relaxation. The relaxed segment was transferred to the recording chamber which was filled with the same relaxing solution, then the vaseline seals were applied and the fiber length in the end pools was cut down to ~500 μm. The length of the voltage-clamped segment of fiber in the central pool was 350 μm. To further improve internal perfusion, the membrane in the end pools was permeabilized either with a brief 2-min protease treatment (trypsin, 0.5 mg/ml in internal solution) or, in later experiments, with a 2-min saponin treatment (0.01% saponin in internal solution) using the protocol of Irving et al. (1987). The solution in the end pools was then exchanged for internal solution (Table I) and the solution in the central pool was exchanged with external solution (Table I), to which a staining concentration of a potentiometric dye (next section) was added. After a staining period of 20–30 min, the central pool was exchanged again with external solution containing a 10–20-fold lower concentration of dye. Currents are expressed as microamps per microfarad of total

fiber linear capacitance ($\mu A/\mu F$). Linear capacitance was computed from the integral of the current transient elicited in response to a 30-mV hyperpolarizing voltage step from a holding potential of −100 mV.

Solutions

The composition of the solutions is given in Table I. The external solution was designed to eliminate all ionic currents and is similar to charge movement recording solutions used by other laboratories. EGTA was included in the internal solution to prevent fiber movement. The concentrations listed for the major salts (K-glutamate, Cs-glutamate, and TEA-SO_4) are approximate and were adjusted slightly to bring the final osmolarity to 235 mosmol for the internal solution, and 255 mosmol for the external solution (±3 mosmol; model 5500 osmometer; Wescor, Logan, UT). We empirically found that it was necessary to keep the osmolarity of the external solution slightly higher than the internal perfusate to prevent swelling of the fiber segment in the central pool. This finding is in qualitative agreement with estimates of the relative osmotic strengths of frog extracellular and cytosolic fluids (Neville and White, 1979; Godt and Maughan, 1988), but differs from results obtained with highly

TABLE I

Solutions

	End pool solutions						
	K-Glu	Cs-Glu	EGTA	PIPES	MOPS	$MgSO_4$	$CaCl_2$
Relaxing	120	0	0.1	5	0	1	0
Internal	0	90	20	0	5	1.35	0.438
	Central pool solution						
	TEA_2SO_4	MOPS	Cs_2SO_4	$CoSO_4$	$CaSO_4$	$MgSO_4$	TTX
External	75	5	5	15	3.25	0.5	1.56

EGTA, PIPES, and MOPS were added as the free acid. The relaxing, internal, and external solutions were titrated to pH 7 using KOH, CsOH, or TEA-OH, respectively. All values are in millimolar except for TTX which is in micromolar.

stretched cut fibers in which no swelling was observed in solutions of matched osmolarity (Irving et al., 1987). We hypothesize that stretch may provide an opposing mechanical force that is not present in our relaxed fibers with average sarcomere length of 2.1 μm. The free Ca concentration of the internal solution was estimated at 10^{-8}, and the free Mg concentration was estimated at 1 mM, using published constants for EGTA, SO_4, and glutamate complexes (Martell and Smith, 1974; Smith and Martell, 1976; Godt and Lindley, 1982). The free Ca concentration of the external solution was ~1 mM.

The external solution also contained one of the following potentiometric dyes: WW-375 (dye XVII of Ross et al., 1977; catalogue No. NK-2495; Nippon-Kankoh Shikiso Kenkyusho Co., Ltd., Okayama, Japan), WW-389 (Dr. A. S. Waggoner, Carnegie Mellon University, Pittsburgh, PA), WW-781 (Molecular Probes, Eugene, OR), RH-155 (catalogue No. NK-3041; Nippon-Kankoh Shikiso Kenkyusho Co., Ltd., Okayama, Japan), or Merocyanine-540 (Eastman Kodak Co., Rochester, NY). For all except Merocyanine-540, a dye concentration of 0.5 mg/ml was used to stain the fibers. For Merocyanine-540, a staining concentration of 0.0125 mg/ml was used. The dyes were added fresh before each experiment and kept in the dark on ice to minimize bleaching. In the case of Merocyanine-540, the solutions were also bubbled with nitrogen to minimize photodynamic damage that occurs with this dye in the presence of

light and oxygen. Control experiments were performed to measure the fiber capacitance and charge movement in the presence and absence of dye. The dyes did not produce any obvious changes in either the linear or voltage-dependent fiber capacitance at the concentrations used in these experiments.

Cobalt, which was included in the external solution to block calcium currents (Horowicz and Schneider, 1981), introduced a measured shift of the charge-voltage curve of 15.5 ± 1.9 mV ($n = 4$); on the other hand, the potentiometric dye WW-375, which is negatively charged, was found to shift the charge-voltage curve -10 ± 0.1 mV ($n = 2$) at the concentrations used in these experiments. Therefore, the net shift of voltage-dependent processes expected for this solution is $\sim +5$ mV.

All experiments were carried out at a temperature of 5°C which was controlled by a peltier device below the chamber.

Optical Methods

The optical recording system was essentially the same as described by Heiny and Vergara (1984). Briefly, the voltage-clamp chamber was mounted on the stage of a compound microscope modified for optical recording. A small spot of quasimonochromatic light was focused by a long working distance objective on the voltage-clamped length of fiber in the central pool, through a glass window in the chamber bottom. The wavelength of the incident light was selected using narrow band interference filters (half bandwidth, 7–14 nm) and exposure times were limited to the recording interval using a digitally controlled electronic shutter. Light transmitted through the illuminated length of fiber in the central pool was collected by a second long working distance objective and focused onto a photodiode. It was converted to voltage and amplified, after subtraction of the constant component contributed by the resting light. The optical signals were measured as the fractional transmittance change, $\Delta I/I$, where ΔI is the change in intensity measured during the test pulse and I is the resting light intensity. These signals were expressed as ΔA using the relation, $\Delta A = -0.43\ \Delta I/I$, which is valid for small intensity changes. Signal-averaging of two to four sweeps per trace was used to improve the signal-to-noise ratio.

The signal from the T-system was selected using unpolarized incident light of wavelength 700 nm. As previously reported for dye WW-375, these illuminating conditions select largely for the absorbance change originating in the T-system membranes. A further enhancement of the signal from the T-system can be obtained using 0° linearly polarized light (Heiny and Vergara, 1984). However, this was not done in the present experiments to avoid the greater signal averaging required with polarized light necessitated by the reduced incident light intensity. Additionally, we found that the absorbance change from the surface membrane, evident as an early rapid step change having the same speed as the voltage-clamp (cf. Figs. 1 and 3), runs down more rapidly than that from the T-system and becomes unresolvable within 20–40 min after the change from the staining to the recording solution. The basis for the faster disappearance of the surface membrane signal may be due to a faster washout of the dye staining the surface membrane. Therefore, except for the data shown in Figs. 1 and 2 in which more signal averaging was used, we simply waited until the surface membrane signal disappeared before recording the T-system signals. We estimate that the maximum surface membrane contribution to the total absorbance change was <10% after the 20–40-min waiting period.

During the time course of an experiment (2–3 h) the dye signals tended to run down as a result of both photobleaching and dye washout from the membrane. Over the recording time of single traces, the rundown was linear and was corrected by fitting and subtracting a sloping baseline from the records (Heiny and Vergara, 1982). Long term decline was monitored periodically at a reference wavelength and pulse amplitude, and was reasonably well fit to a single

exponential that was used to correct all traces. Additionally, paired hyperpolarizing and depolarizing records were always taken close together in time, and control experiments were performed which verified that the findings reported were independent of the order in which the pulses were applied.

Pulse Generation and Data Acquisition

Pulses were applied and data were acquired digitally using a custom-built programmable pulse generator and data acquisition system based on an IBM-AT microcomputer (modified UCLA-WAD system, Axon Instruments, Inc., Burlingame, CA). The A/D and D/A were both single-channel units with a resolution of 12 bits. Optical and current records were acquired sequentially at each test potential by switching the input to the A/D. All bits and control pulses to the set-up were opto-isolated from the digital ground to reduce noise. For most experiments, the command pulse to the voltage clamp was filtered at 5 kHz using a programmable 8-pole Bessel filter. Similar filters in front of the A/D inputs limited the final signal bandwidth to 1–2 kHz.

T-System Model Simulations

The predicted current transients and T-system light signals were modeled using a distributed cable equivalent circuit model of the T-system. Eq. 9 of Adrian et al. (1969) was expressed in finite difference form using an implicit Crank-Nicholson approximation, and solved numerically for the boundary conditions of a voltage-clamped surface membrane with a small access resistance at the tubular openings (Adrian and Peachey, 1973). The radial computation interval, Δr, was set at 1/16 the fiber radius, which effectively divided the T-system into 16 concentric disks, each containing resistive and capacitive elements proportional to the membrane area of that disk. The details of the numerical calculation are as described previously (Ashcroft et al., 1985). This computation yields the predicted current density as a function of time, $I_m(t)$, at the surface membrane and the predicted T-system potential, $V_T(r, t)$, under passive linear conditions. The predicted weighted average T-system potential change, $\langle V_T(t) \rangle$, was computed by summing the T-system potential at each disk, weighted by the membrane area of that disk. If all of the absorbance signal represents a response to the T-system transmembrane potential change, then $\langle V_T(t) \rangle$ is directly comparable with our measured T-system optical signals (Heiny and Vergara, 1984; Ashcroft et al., 1985).

The definitions for the morphological and passive membrane constants used in these calculations follow those given in Adrian et al. (1969) and Adrian and Peachey (1973). The values used were: $\rho = 0.003$, $\zeta = 10^{-6}$ cm, $\sigma = 0.5$, where ρ is the fractional fiber volume occupied by the T-system, ζ is the volume to surface ratio of the tubules, and σ is a network factor that describes the degree of isotropy of the T-system cross-sectional geometry at the branch points for current flow. The specific capacitance of the T-system (C_W) was set at 1 μF/cm^2. The lumen conductivity (G_L) was set at 0.011 S/cm, which is the measured conductivity of our external solution. The access resistance (R_A) was varied from 10–50 Ω-cm. It was found empirically that these low access resistance values and a T-system lumen conductivity equal to the measured conductivity of the external solution, gave a good fit to the T-system optical transients (Ashcroft et al., 1985; and this paper). Values for the specific wall conductance of the T-system, G_W (S/cm^2), and the fiber radius (cm) were adjusted for each fiber. Fiber diameters were measured with a compound microscope at 200 power, and are given for each fiber in the figure legends. Our large diameter fibers were typically ellipsoid in cross section and were mounted in the chamber with the major axis in the plane of focus. Because the model assumes a circular cross section, the value for the radius used to compute the simulated traces was adjusted assuming that the measured value overestimates the cross-sectional area by 25% (Dulhunty and Gage, 1973).

To obtain the predicted T-system response at voltages which activate charge movement, we included in each disk a voltage- and time dependent capacitance based on the model of Chandler et al. (1976*a*). In this model, a single charged species (Q) is assumed to move between two states (resting and active), with forward and reverse rate constants (α and β) that are single-valued functions of voltage (V), according to the relations:

$$Q_{\text{rest}} \underset{\beta(V)}{\overset{\alpha(V)}{\rightleftharpoons}} Q_{\text{active}} \tag{1}$$

$$\alpha(V) = \frac{C(V - \bar{V})/k}{1 - \exp[(V - \bar{V})/k]} \tag{2}$$

$$\beta(V) = \frac{-C(V - \bar{V})/k}{1 - \exp[(V - \bar{V})/k]} \tag{3}$$

where C is an adjustable constant (ms^{-1}), $\bar{V}$ is the midpoint of the charge-voltage distribution, and k is a slope factor (mV^{-1}).

The specific density of charge movement in the T-system, Q_w (nC/cm^2), was adjusted to give a total peak charge movement Q ($nC/\mu F$) matching the measured value. The overall rate constants, $\tau(V)$, were obtained by fitting the decay of the charge movement transients at each voltage to a single exponential, after subtraction of the steady-state leak current, and were performed for the experiment of Fig. 7. These were fitted to the equation $\tau(V) = \alpha(V) + \beta(V)$. Values for $\bar{V}$ and k were taken from the steady-state charge-voltage distribution measured in the same fiber and fitted to a single two-state Boltzmann function. The only adjustable parameter was the factor C (ms^{-1}). The fits described above were performed using a least-squares method based on the algorithm of Brown and Dennis (1972).

Although at least two components contribute to the measured charge movement currents, the single two-state model used here was considered adequate for the purpose of estimating the effect of the additional nonlinear capacitance on the time course of the T-system charging transient. This calculation was performed at a single large applied potential at which the decays of the two components merge together (cf. Figs. 7 and 8). The time course of the predicted weighted-average T-system potential change was compared with the T-system optical transient of Fig. 7, which was obtained at the same potential.

Comparisons of the overall model predictions, $I_m(t)$ and $\langle V_T(t) \rangle$, with the measured current and light traces were judged by eye. Because the calculation depends on a large number of membrane constants it was not considered worthwhile to perform a detailed least-squares fit of the model to the data; the fitted parameter values would not be uniquely determined and such calculations are impractical on our microcomputer. We used published values that were reasonably well determined for most of the T-system membrane constants, then adjusted the fiber radius and wall conductance for each fiber. This was adequate for the purposes of the comparisons made in Figs. 3 and 9 of this study.

RESULTS

Dye Controls

Dye WW-375 belongs to the merocyanine-rhodamine class of voltage-sensing dyes which have been shown to act as rapid, linear probes of transmembrane potential in a wide variety of tissues and recording conditions (Ross et al., 1977; Cohen and Salzberg, 1978; Gupta et al., 1981). In skeletal muscle, because the dye is nonpenetrating and stains all membranes accessible to the extracellular solution, the optical signals recorded with this dye contain contributions from both the surface and

T-system membranes. A careful analysis of the action spectrum of this dye in skeletal muscle and its relationship to the physico-chemical mechanisms of the dye response has shown that it is possible to identify and separate the contributions of the surface and T-system membranes to the total optical signal (Heiny and Vergara, 1982, 1984).

We performed control experiments to determine if the response of this dye under charge movement recording conditions was similar to that previously reported using more physiological salt solutions. Fig. 1 shows optical signals recorded at two wavelengths from a voltage-clamped muscle fiber stained with dye WW-375 and perfused internally and externally with solutions designed to eliminate all ionic currents (Table I). The wavelengths chosen correspond to those at which the largest signal from either the surface (740 nm, right traces) or T-system membrane (700 nm, left traces) was found in previous studies. The signals were recorded in response to the same 60-mV hyperpolarizing voltage-clamp pulse, from a holding potential of −100 mV; additionally, the signals at each wavelength were recorded in response to pulse durations of both 1 ms (top traces) and 15 ms (lower traces). As can be seen, two signal components contribute to the absorbance change at each wavelength. There

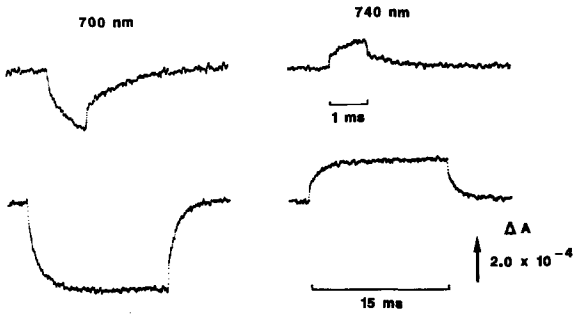

FIGURE 1. Absorbance signals recorded at two wavelengths and pulse durations, from a muscle fiber stained with dye WW-375 and pulsed to −160 mV. Fiber diameter, 108 μm.

is an early fast signal component (top, right) that rises within 60 μs, which is the speed of the applied voltage-clamp step in these experiments; as shown previously, this component is contributed by the surface membrane and is largest at 740 nm. There is also a slower component that is best seen in the longer duration records (lower traces); this component has a time course compatible with its arising from the voltage change in the T-system which lags the applied voltage step, and is largest at 700 nm.

These results indicate that the wavelength-dependent separation of surface and T-system membrane signals previously reported for this dye is not significantly altered by the recording conditions of these experiments.

To further analyze the spectral properties of the dye in these conditions, we measured the action spectra of the separate surface and T-system signals over the entire absorption band. Fig. 2 shows the action spectra recorded from a fiber illuminated with unpolarized quasimonochromatic light from 600–800 nm, and stimulated with the same −60-mV voltage-clamp pulse. The surface membrane signal (+) was defined as the absorbance change at 60 μs and was measured using short 1-ms pulses with more extensive signal averaging (32 sweeps); the T-system signal (*open*

circles) was defined as the steady-state absorbance change at 30 ms less the surface membrane signal, and was obtained using longer duration pulses (see inset). As can be seen, the action spectrum of the signal from both membranes is triphasic, with negative absorbance peaks at 650 and 700 nm, and a positive absorbance peak at 740 nm; the T-system signal is largest at 700 nm, whereas the surface membrane signal is largest at 740 nm. Similar spectra were obtained in two additional fibers.

Comparison of these spectra with those obtained previously (Heiny and Vergara, 1982, 1984) indicates that the spectral properties of the potential-dependent response of dye WW-375 are essentially similar in both solutions. From this result we can also infer that the mechanism of the potential-dependent response of WW-375 is not significantly different under these conditions.

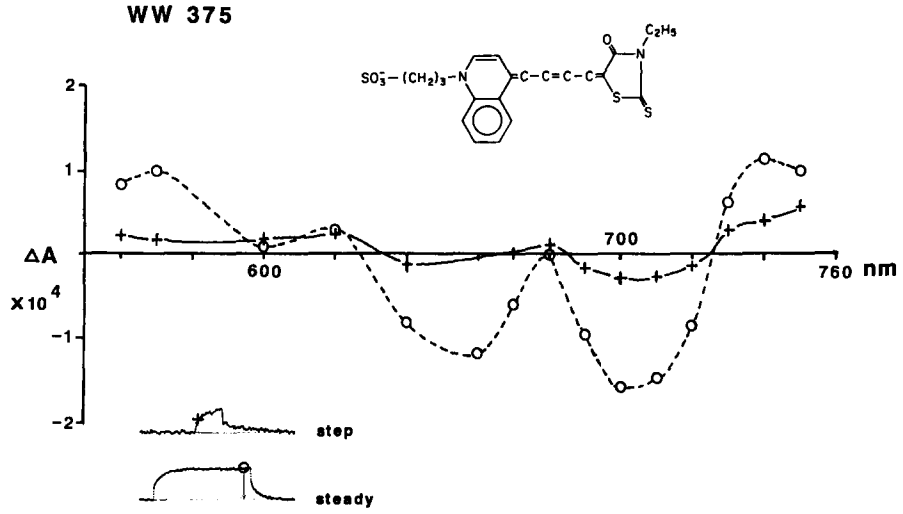

FIGURE 2. Action spectra of the absorbance signals contributed by the surface (+) and T-system (O) membranes stained with dye WW-375. The absorbance change contributed by the surface membrane was measured as the amplitude of the step component at 60 μs. The absorbance change contributed by the T-system was measured as the steady-state amplitude at 30 ms, less the step component (see inset). The lines through the data points were drawn by eye.

Quality of Voltage-Clamp Control of the T-System

We used the T-system signal at 700 nm to examine the passive behavior of the T-system in these solutions under a variety of conditions. Fig. 3 examines the time course of passive charging of the T-system in response to a hyperpolarizing test pulse from −100 to −170 mV. The top trace shows the membrane potential recorded with the voltage clamp; the middle trace is the T-system light signal; the lower trace is the membrane current. In this voltage range, nonlinear membrane phenomena should be absent, and the T-system light signal should reflect solely the passive electrical behavior of the T-system. As shown, the voltage recorded at the surface membrane settles to a constant amplitude in 60 μs. As expected, the T-system light signal lags the surface membrane potential. However, after an initial

charging time of 4 ms (measured at 95% of the final value), the T-system light signal is constant. In 14 fibers, the mean time for the optical signal to reach a steady level was 3.7 ± 0.2 ms (range 2.5–6 ms), for fibers of mean diameter of 129.3 ± 5.6 μm.

It should be noted that the light signal from the T-system represents a weighted average of potential changes occurring along the entire fiber radius. Therefore, the absorbance change contributed by the T-system potential at each radial position will be proportional both to the potential and the amount of membrane at that radial position. Since there is more T-system membrane in an annulus near the edge than near the center of the fiber, potential changes near the edge of the fiber will contribute proportionately more to the total optical signal. For these reasons, the optical signal at early times reflects predominantly the time course of the more rap-

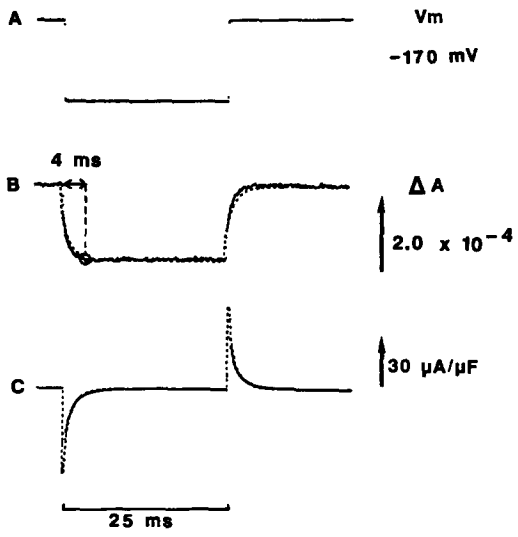

FIGURE 3. (*A*) Membrane potential recorded with the voltage clamp. (*B*) T-system absorbance signal recorded with dye WW-375 at 700 nm; the 95% point is indicated by circle. (*C*) Membrane current. The continuous lines are the fiber responses elicited with a hyperpolarizing applied potential step to −170 mV from a holding potential of −100 mV. The dashed lines through traces *B* and *C* are the predicted weighted average T-system potential change, $\langle V_T(t) \rangle$, and predicted membrane current, computed using a radial cable equivalent circuit model of the T-system (see text). Sampling rate, 40 μs/point. Fiber diameter, 110 μm. The adjustable parameters used in the model simulation were: R_A = 10 Ω-cm, G_W = 2.2 μS/cm², radius = 50 μm.

idly charging outer regions of the T-system. The data of Fig. 3 indicates, however, that after an initial charging time, the potential of all regions of the T-system, including the more slowly charging regions at the center of the fiber, is constant. At this time, because of the high membrane resistance expected in these solutions, steady state differences in potential along the radius should be small and the T-system potential at every point should approach the command potential.

The quality of space-clamp control in the T-system in the steady-state can be evaluated by calculating some limiting values for the T-system space constant. A lower boundary can be estimated from the measured steady-state membrane current in this fiber, which was 1.0 μA/μF. If we assign all of this current to ionic conductances, which is likely to be an upper limit since leak currents across the vaseline seals contribute a small component, the fiber membrane resistance is at least 10

$k\Omega\text{-}cm^2$, referred to the outer membrane surface. A specific resistance of this magnitude in the T-system would give a radial space constant of at least 70 μm, which would produce a maximum steady-state potential decrement of 15% at the center of a 100 μm fiber. The actual specific membrane resistance and space constant of the T-system in these solutions are likely to be much greater.

We can also compare the light and current records to the signals predicted from a radial cable model of the T-system to obtain an independent estimate of the actual radial space constant under these conditions. For example, using the model and constants given in Methods, it was possible to obtain a reasonable prediction for the T-system light signal and simultaneously fit the capacity transient measured from the same fiber, assuming a specific T-system membrane conductance, G_w of 2.2 $\mu S/cm^2$.

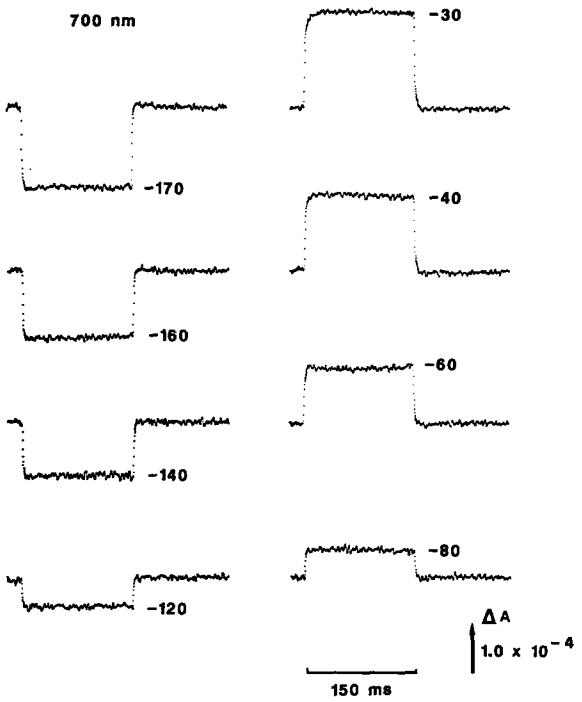

FIGURE 4. T-system absorbance signals elicited in response to imposed steps to the indicated potential, from a holding potential of −100 mV. Dye WW-375, 700 nm. Fiber diameter, 110 μm.

These predicted transients are shown in the dashed lines of Fig. 3, *B* and *C*. For five additional fibers analyzed in this way, the adjusted values of G_w ranged from 2–20 $\mu S/cm^2$. These values agree reasonably well with estimates of 3–7 $\mu S/cm^2$ for the specific T-system membrane resistance in passive solutions, obtained from an analysis of the effective membrane capacity (Adrian and Almers, 1974). This range of G_w values corresponds to a radial space constant of 135–400 μm, or about two to eight fiber radii. The lowest (worst case) value predicts a maximum steady-state potential decrement from the edge to the center of the fiber of 3.5%. These results taken together indicate that a good space clamp of the T-system is achieved under these conditions in the steady-state, as expected.

Fig. 4 examines the T-system absorbance signals elicited in response to a range of

both hyperpolarizing and depolarizing voltage steps. In addition, the pulses were extended to 150 ms duration in order to examine the T-system voltage over recording times typically used for charge movement measurements.

It can be seen that the T-system light signal elicited with hyperpolarizing pulses (Fig. 4, left traces) increases in an approximately linear manner with increasing hyperpolarization, and remains constant for the duration of the pulse. Similar results are seen in the depolarizing direction, where the direction of the absorbance change is reversed (Fig. 4, right traces). However, a closer comparison of paired hyperpolarizing and depolarizing light signals reveals some differences in their kinetics and amplitude. The light signal recorded in the hyperpolarizing direction reaches a steady level within a few milliseconds at all potentials. In contrast, the light

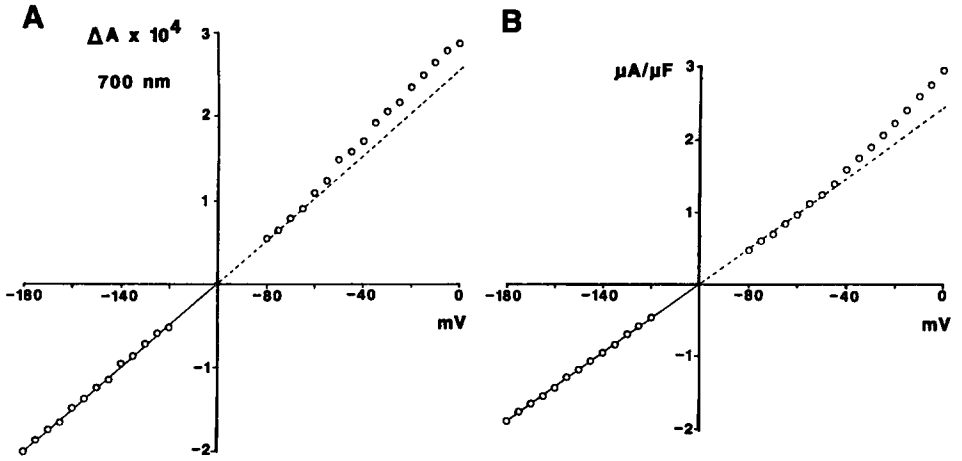

FIGURE 5. (*A*) Steady-state T-system absorbance change (O) vs. command potential (millivolts). The steady-state absorbance change was measured at the end of a 150-ms pulse. It was computed as the mean value during the last 6 ms at the pulse end, minus the mean value during the 6 ms before the pulse start. The solid line was fitted through the hyperpolarizing data points (fitted slope, 2.53×10^{-6} $\Delta A/mV$; correlation coefficient, 0.999). The dotted line is the extrapolation of the same fitted line to positive potentials. (*B*) Steady state current at 150 ms (O) vs. command potential, from the same fiber. The solid line was fitted through the hyperpolarizing data points (fitted slope, 0.024 $\mu A/\mu F$ per mV; correlation coefficient, 0.999). Dye WW-375, 700 nm. Fiber diameter, 115 μm.

signals elicited with depolarizing pulses to -40 and -30 mV take up to 20 ms to reach a constant amplitude; moreover, this amplitude is larger than that of the equivalent hyperpolarizing pulse. These differences are examined in more detail in the following figures.

Fig. 5 *A* examines the relationship between the steady-state T-system light signal, and the command potential applied at the surface membrane. It is apparent that this relationship is not completely linear, as expected for a purely passive membrane. The hyperpolarizing data points and the depolarizing data below ~ -60 mV can be well fit with a single straight line. However, at larger depolarizations the data deviate from the fitted line. This deviation appears to saturate at large depolarized

potentials and at −20 mV represents an absorbance increase of 22% with respect to the fitted line. The mean percent increase in 17 fibers examined was 17.8 ± 3.3% (SD).

Fig. 5 *B* compares the corresponding steady-state current-voltage relationship to examine whether the nonlinearity in the T-system light signal could be explained by lack of voltage-clamp control in the T-system caused by residual unblocked ionic currents. A problem with voltage-clamp control in the T-system would necessarily be associated with nonlinearities in the current-voltage relationship.

In this fiber, the current-voltage relationship was linear at potentials below ~−55 mV. However, above this voltage we detected a small outward current which we attribute to residual ionic currents that are not entirely blocked in these solutions.

It should be noted that the steady-state current plotted in Fig. 5 *B* includes current from all sources, i.e., ionic currents from both the surface and T-system, and leak currents across the vaseline seals (at voltages near the mechanical threshold there may also be a small contribution from Q_γ charge movement which has very slow kinetics in this voltage range; Adrian and Huang, 1984). The current for paired hyperpolarizing and depolarizing traces can be added to isolate the net nonlinear ionic current. When this was done for the fiber in Fig. 5 *B*, the net ionic current above −55 mV was outward, and reached an amplitude of 0.34 μA/μF at −20 mV.

In other fibers, the net nonlinear ionic current was variable in both polarity and amplitude. The extra current ranged from essentially unmeasurable to a maximum of ±0.5 μA/μF at −20 mV. It could be either outward or inward depending on the fiber and the potential. This contrasts with the nonlinear optical signal which was an absorbance increase over the same voltage range in every fiber.

In considering whether these residual ionic currents could cause the T-system potential to deviate from voltage-clamp control, we first note that, for the fiber in Fig. 5, the direction of the residual current is opposite that which would be required to drive the T-system to a larger amplitude than the applied potential; to do this in this voltage range would require an active conductance generating an inward current.

For fibers in which a net inward current was detected in this voltage range, we can test whether a current of the magnitude detected would be sufficient to cause the T-system to escape from voltage-clamp control and drive the T-system to more positive values by ~10–20 mV. We first compared this inward current with previous studies of the extent to which the T-system potential deviates from linearity under conditions in which an active T-system conductance was intentionally left unblocked. For example, when the sodium conductance of the T-system is activated, local sodium currents can drive the T-system potential to a value larger than the applied step potential, setting up a positive feedback loop which causes the T-system to escape from voltage-clamp control (Vergara and Bezanilla, 1981; Heiny and Vergara, 1982). Under such conditions, it is possible to have a large potential change in the T-system that is not associated with a correspondingly large current density supplied by the voltage clamp. In this case, a pulse to −50 mV produced an extra late sodium current from the T-system ("notch") of ~10 μA/μF that was sufficient to cause the potential of the T-system to escape from voltage-clamp control and

approach the sodium equilibrium potential. This measured radial current was two orders of magnitude greater than the residual currents detected in the present study using passive solutions, over the voltage range where the extra absorbance signal occurs. It is also possible to calculate theoretically the minimum active current from any source that would be required to drive the T-system more positive by 20 mV. We performed this calculation numerically using the model described previously, to which was added an arbitrary active conductance of general form (i.e., time-independent activation and equilibrium potential set positive to the command potential to give inward current). The calculation was relatively insensitive to a range of values assumed for the passive T-system membrane constants, except for the access resistance parameter; for values of access resistance ranging from 0 to 150 Ω-cm, a predicted radial current density of 10–30 $\mu A/\mu F$ measured at the surface membrane by the voltage clamp was required for the weighted average T-system potential to show a positive deviation as large as 20 mV. Again, both the measured and predicted values are one to two orders of magnitude larger than any current we detect.

We also considered the possibility that some residual unblocked passive conductance might be present in the T-system. Another way it might be possible to obtain a depolarizing voltage change in the tubules larger than the equivalent hyperpolarizing response is if there were some unblocked passive conductance in the T-system that was turned on in the hyperpolarizing range of potentials. In this case, the T-system would charge to a smaller average potential in the hyperpolarizing direction compared with the equivalent depolarizing pulse, which results in an apparent extra depolarization when paired optical traces are compared. The net ionic current obtained by adding paired depolarizing and hyperpolarizing currents at each voltage would be inward. We can compare the present results with previous studies of the inward rectifier conductance of the T-system (Ashcroft et al., 1985), in which it was shown that a specific membrane conductance of 0.5 mS/cm^2 in the T-system was required to attenuate the optically measured hyperpolarizing T-system voltage transient by 20–30% (equivalent to 10–20 mV transmembrane potential change). A conductance of this magnitude in the T-system would produce a radial current density of 100–300 μA per square centimeter of surface membrane (or 10–30 $\mu A/\mu F$), measured with the voltage clamp. In the passive solutions used here, the inward rectifier is largely blocked by Cs and TEA, and the maximum net inward current is one to two orders of magnitude less than that required to alter the T-system voltage by 10–20 mV.

The same arguments hold for possible unblocked agonist-activated conductances. It is possible to propose, for example, that calcium released from the sarcoplasmic reticulum at depolarizing potentials might activate calcium-dependent conductances in the T-system. However, any conductance, irrespective of how it is initially turned on, would be expected to produce ionic current which should be detected by the voltage clamp.

We conclude that the residual ionic currents detected under these conditions are not sufficient to produce changes in the weighted average T-system potential of the magnitude indicated by the extra absorbance signal. Taken together, these results suggest that the nonlinearity in the T-system light signal cannot be explained by voltage decrements or escape of voltage-clamp control in the T-system.

Dependence of the Nonlinear Signal on Holding Potential

Fig. 6 examines the dependence of the T-system absorbance change on the holding potential. In this case, the membrane potential was stepped positive and negative to the indicated potential, from a holding potential of either −100 (*open circles*) or 0 mV (*filled circles*).

As can be seen, the absorbance change recorded in response to voltage steps from a holding potential of −100 mV deviates from linearity in the voltage range of −80 to −20 mV, which is similar to that shown in Fig. 5. In contrast, when the membrane is stepped from a holding potential of 0 mV, these deviations disappear and the response is linear over the entire voltage range explored, including the same range where the extra response was observed from the normal holding potential. When the line fit through the hyperpolarizing data points (*solid line*) was extrapolated to positive potentials (*dashed line*), the depolarizing data points fell entirely on this line. Moreover, the fitted slope factor was not significantly different from that which fit the hyperpolarizing data obtained with the −100-mV holding potential. This phenomenon is reversible; if the holding potential is returned to −100 mV (not shown), the nonlinearities in the absorbance response reappear.

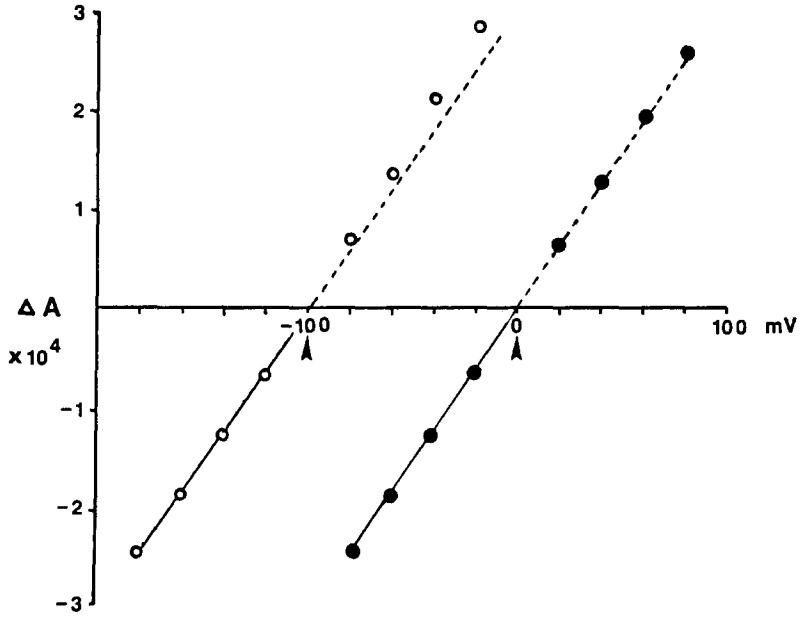

FIGURE 6. Steady-state T-system absorbance change vs. command potential (millivolts), for two different holding potentials. The fiber was stepped to the indicated potential from a holding potential of either −100 mV (*open circles*) or 0 mV (*filled circles*). The solid lines were fitted through the hyperpolarizing data points. For the data points taken from the −100 mV holding potential, the fitted slope factor was 3.12×10^{-6} ΔA/mV (correlation coefficient, 0.999). The dotted line is the extrapolation of the fitted line to positive data points. For the data points taken from the 0-mV holding potential, the fitted slope factor was 3.14×10^{-6} ΔA/mV (correlation coefficient, 0.999). Dye WW-375, 700 nm. Fiber diameter, 125 μm.

In considering whether some dye-related artifact might be responsible for the extra absorbance signal, it is relevant that in the voltage range of −80 to −20 mV the dye is being challenged to sense the same absolute membrane potential in both cases, the only difference being that the two measurements start from different holding potentials. It is difficult to postulate a dye-related process in which the dye could "know" the initial conditions. On the other hand, a number of membrane-related processes are known to exist that inactivate in a voltage-dependent manner. For these reasons it seems unlikely that the extra absorbance signal is an artifact of the dye response, or for that matter of something else in the protocol or light-measuring system. These considerations, combined with the finding that the same dye gives a linear response to potential in the surface membrane (Heiny and Vergara,

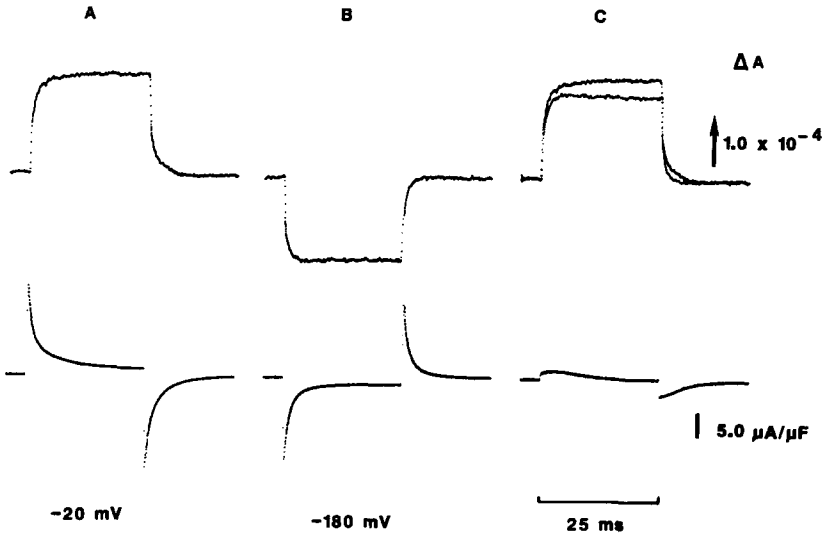

FIGURE 7. T-system absorbance signals (*top traces*) and membrane current (*lower traces*) recorded for potential steps of 25-ms duration to −20 mV (*A*) and −180 mV (*B*). The top of *C* superimposes the depolarizing and inverted hyperpolarizing absorbance traces, for comparison. The lower part of *C* shows the difference membrane current (*A* plus *B*). Dye WW-375, 700 nm. Same fiber as Fig. 3.

1982), suggest that the extra absorbance change reports a T-system membrane-related phenomenon.

Comparison with Charge Movement

The extra absorbance change has several features that suggest a correlation with mechanical activation. It appears in the same voltage-range as charge movement and mechanical activation. Similarly, it disappears after prolonged depolarization as do both charge movement and the mechanical response of muscle fibers (Hodgkin and Horowicz, 1960; Chandler et al., 1976*a*, *b*; Adrian et al., 1976). Therefore, we compared the optical traces with charge movement currents recorded from the same fiber.

Fig. 7 compares the absorbance signals and currents at early times, from a fiber

held at −100 mV and pulsed to −20 mV (Fig. 7 *A*) and −180 mV (Fig. 7 *B*). The top traces in *C* show the hyperpolarizing light signal inverted and superimposed with the depolarizing light trace for comparison; the lower trace shows the net nonlinear current (*A* plus *B*), which reveals the voltage-dependent charge movement. As noted above, the depolarizing light signal (Fig. 7 *A*, top) takes longer to reach a constant level than the corresponding hyperpolarizing transient (Fig. 7 *B*, top). Likewise, it returns more slowly to the baseline when the pulse is turned off. It is apparent that these kinetic differences correlate with similar differences in the speed of the corresponding capacity transients (Fig. 7, lower traces, *A* and *B*).

A parallelism between the time course of the current decay and the light signals is expected since the current transients reflect the current that is charging the T-system to the new potential. In this case, the observed kinetic differences between depolarizing and hyperpolarizing traces are also expected since the fiber capaci-

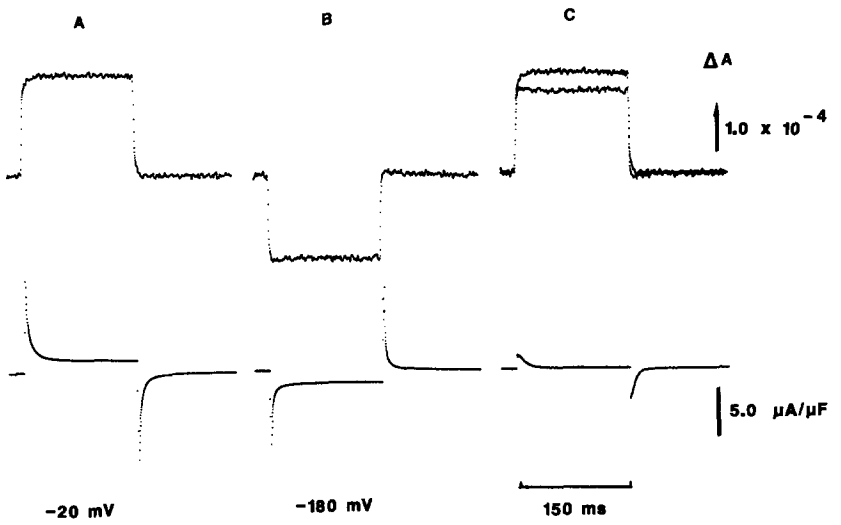

FIGURE 8. Same fiber and protocol as Fig. 7, but for pulse durations of 150 ms.

tance at −20 mV is greater than at −180 mV, which is because of the extra voltage-dependent capacitance contributed by charge movement. We chose −20 mV for this comparison because it is near the midpoint of the charge-voltage distribution, where the voltage-dependent capacitance is maximum.

Fig. 8 shows the same comparisons for a longer pulse duration. It can be seen that the extra absorbance signal remains constant for the duration of the pulses, after the charge movement current transient has decayed. Again, there is no correlation between the extra light signal and unblocked ionic currents, which in this fiber were less than 0.03 μA/μF at the pulse end (Fig. 8 *C*, lower).

From these data, it is apparent that kinetic differences on the light signal appear at approximately the same time as charge movement appears, whereas amplitude differences remain after the charge movement current has decayed.

We can compare this finding qualitatively with the electrical response expected for a membrane that contains a voltage-dependent capacitance. Activation of a volt-

age-dependent charge movement is expected to slow both the capacity transient and the T-system voltage transient. However, it is not expected to alter the steady-state T-system voltage or to drive it to a larger potential. Charges confined to move within a dielectric are inherently "nonelectrogenic." By analogy with a lossy capacitor, such charges are expected to rotate to oppose an applied field, thereby reducing the net voltage across the capacitor; in the case of a voltage-clamped membrane, the voltage clamp supplies the extra current to bring the potential back to the command potential.

To obtain a more quantitative estimate of the effect of charge movement on the

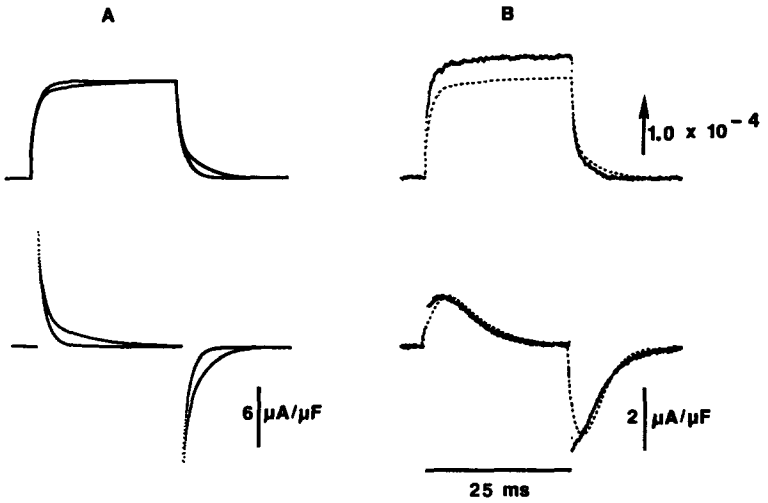

FIGURE 9. (*A*) (*Top traces*) predicted weighted average T-system potential change, $\langle V_T(t) \rangle$, for hyperpolarizing and depolarizing applied potential steps of ±80 mV from the holding potential. (*Lower traces*) the corresponding predicted membrane current transients. The hyperpolarizing voltage and current traces are shown inverted, and are the faster transients of each pair. (*B*) The top traces compare the depolarizing optical transient of Fig. 7 *A* (*continuous line*) with the predicted depolarizing weighted average T-system potential change (*dashed line*). The lower traces compare the observed charge movement transient of Fig. 7 *C* (*continuous line*) with the predicted charge movement transient (*dashed line*). The adjustable parameters used in the model simulation were: R_A = 10 Ω-cm, G_W = 2.2 μS/cm², radius = 50 μm, Q_W = 60 nC/cm², $\bar{V}$ = −35 mV, k = 8.5 mV, C = 0.065 ms⁻¹, Q = 250 nC/cm² (27 nC/mF).

time course of the T-system charging transient at depolarized potentials, we compared these traces with those predicted by a radial cable model of the T-system that included a voltage- and time-dependent capacitance. Parameters were chosen to give predicted optical and current transients that closely matched those shown in Fig. 7, as described in Methods. The predicted hyperpolarizing optical and current traces for this fiber were shown in Fig. 3 and gave a prediction reasonably close to the passive T-system membrane response of this fiber. These same fitted traces are shown inverted in Fig. 9 *A* (the faster signals of each pair) and compared with the optical and current traces predicted for the same fiber at a depolarizing potential of

−20 mV (the slower traces of each pair). As noted previously, the charging time of ~4 ms obtained from the hyperpolarizing optical data is close to that predicted for a fiber of this diameter in passive solutions. From this comparison, it can also be seen that the slower charging time observed in the depolarizing optical data is consistent with what is expected from a membrane having a nonlinear capacitance with parameters close to those measured for charge movement. In this simulation, the time for the T-system to reach 95% of its final value was 8 ms. This kinetic difference between the depolarizing and hyperpolarizing optical transients is expected because the T-system cable is not isopotential under non–steady-state conditions and cannot be rapidly voltage clamped. However, it can also be seen that a cable having these electrical properties is expected to charge to the same steady-state amplitude as the applied potential, for both pulse polarities. Fig. 9 *B*, top, compares this predicted weighted average T-system potential change (*dashed line*) with the observed depolarizing optical transient (from Fig. 7 *A*). The time course of the observed optical transient parallels the predicted T-system signal. However, after the first few milliseconds, its amplitude is greater by an approximately constant amount. This difference disappears when the membrane is repolarized. This difference represents the component of the depolarizing optical signal that is not expected for the charging transient of the T-system in the presence of charge movement. Fig. 9 *B*, lower, shows the predicted current traces of Fig. 9 *A*, subtracted, to reveal the predicted charge movement (*dashed trace*). The latter reproduces most of the features of the observed transient of Fig. 7 *C* (*continuous trace,* shown here at higher gain), after the first few milliseconds. The actual charge movement transient has multiple components, including an early fast component, that is not reproduced by the simple two-state model used here, and will also affect the time course of the predicted T-system charging transient, $\langle V_T(t) \rangle$.

In summary, kinetic differences in the T-system charging time are expected from a membrane with charge movement, whereas amplitude differences are not. The observed kinetic differences between depolarizing and hyperpolarizing optical signals are quantitatively consistent with the parameters of charge movement, and therefore these differences can be largely attributed to charging delays produced by charge movement. However, charge movement itself could not produce an extra depolarization and we must consider alternative hypotheses for the origin of the extra nonlinear absorbance change.

Location of the Extra Absorbance Change

The most likely proposal is that the extra absorbance signal reports some local change in electrostatic potential in or near the T-system membranes. The latter would exist only inside the bilayer or within molecular distances of the membrane, and would not be controlled by the voltage clamp which responds solely to the potential of the bulk solution. On the other hand, potentiometric dyes are probes of molecular dimensions and they readily associate with membranes. A response to both the bulk transmembrane potential and to local electrostatic potentials is necessarily expected for any charged or dipolar molecule that partitions in the membrane and whose spectral properties are sensitive to the microenvironment. In fact, a large body of experimental data demonstrates that the spectral properties of most poten-

tiometric dyes, in addition to their well-characterized responses to bulk transmembrane potentials, are sensitive to local electrostatic potentials (Aiuchi and Kobatake, 1979; Russell et al., 1979; Krasne, 1980, 1983; Beeler et al., 1981).

Therefore, we repeated these experiments with other potentiometric dyes whose chromophores have different structures, charge distributions, and permeabilities in lipid bilayers. We chose two additional merocyanine dyes, WW-389 and Merocyanine-540 (Cohen et al., 1974; Ross et al., 1977), and two oxonol dyes, WW-781 (Gupta et al., 1981) and RH-155 (Grinvald et al., 1986) whose structures are shown in Fig. 10. All are reported to be fast response, nonpenetrating potentiometric probes, but sense membrane potential by different mechanisms (Waggoner and Grinvald, 1977; Waggoner, 1979). A schematic of the proposed mechanisms of action, summarized from the work of other laboratories, is shown to the right of each dye. For each of the dyes tested, it was possible to find a T-system signal component having a time course comparable to that shown for dye WW-375 (Fig. 3) in response to hyperpolarizing pulses. The wavelength used was that which gave the largest T-system signal. It should also be noted that the signals from each of the dyes displayed kinetic differences (not shown) similar to those reported in Figs. 7 and 8 for dye WW-375, and that the steady-state membrane current recorded from fibers stained with these dyes showed a linear voltage dependence, similar to that shown in Fig. 5 *B* for dye WW-375. We next examined whether these dyes reported differences in steady-state amplitudes between depolarizing and hyperpolarizing pulses, similar to that found with dye WW-375 (Fig. 5).

Merocyanine-540 (M-540) was tested because it is the most extensively characterized of the merocyanine dyes. The merocyanine molecule (Fig. 10) has a single negative charge at the sulfonate end that partitions in the aqueous phase and renders it membrane impermeant, and a hydrophobic chromophore of delocalized charge and high dipole moment (~10 Debye) which readily associates with membranes (Wolf and Waggoner, 1986). The fixed charge is confined to the aqueous phase and serves as a pivot point for rotation of the chromophore; spectral changes result from a potential-dependent shift of a dynamic equilibrium between monomeric dye molecules oriented with the long axis of the chromophore perpendicular to the membrane, and dimerized molecules oriented parallel to the surface of the bilayer (Warashina and Tasaki, 1975; Waggoner and Grinvald, 1977; Dragsten and Webb, 1978; Waggoner, 1979; Wolf and Waggoner, 1986). The results obtained with M-540 are shown in Fig. 11 (left plot) and are similar to that reported for dye WW-375, although the absolute magnitude of the signals is smaller due to the hundredfold lower dye concentrations used. Nevertheless, a large extra absorbance change is observed at depolarized voltages. In this fiber, the absorbance change at −20 mV was 21% larger than the fitted line; on average, the mean percent increase in three fibers was 23 ± 2% (SD).

Dye WW-389 was also tested because it is a close merocyanine-rhodamine analogue of dye WW-375. The merocyanine-rhodamine dyes belong to the same general class of dyes as Merocyanine-540. They also have a hydrophobic, dipolar chromophore and, most likely, sense potential by similar mechanisms (Wolf and Waggoner, 1986). Dye WW-389 has a butyl in place of the ethyl side chain, which is expected to render it more lipophilic. The results with dye WW-389 (not shown; 700 nm) were indistinguishable from those shown in Fig. 5 for dye WW-375.

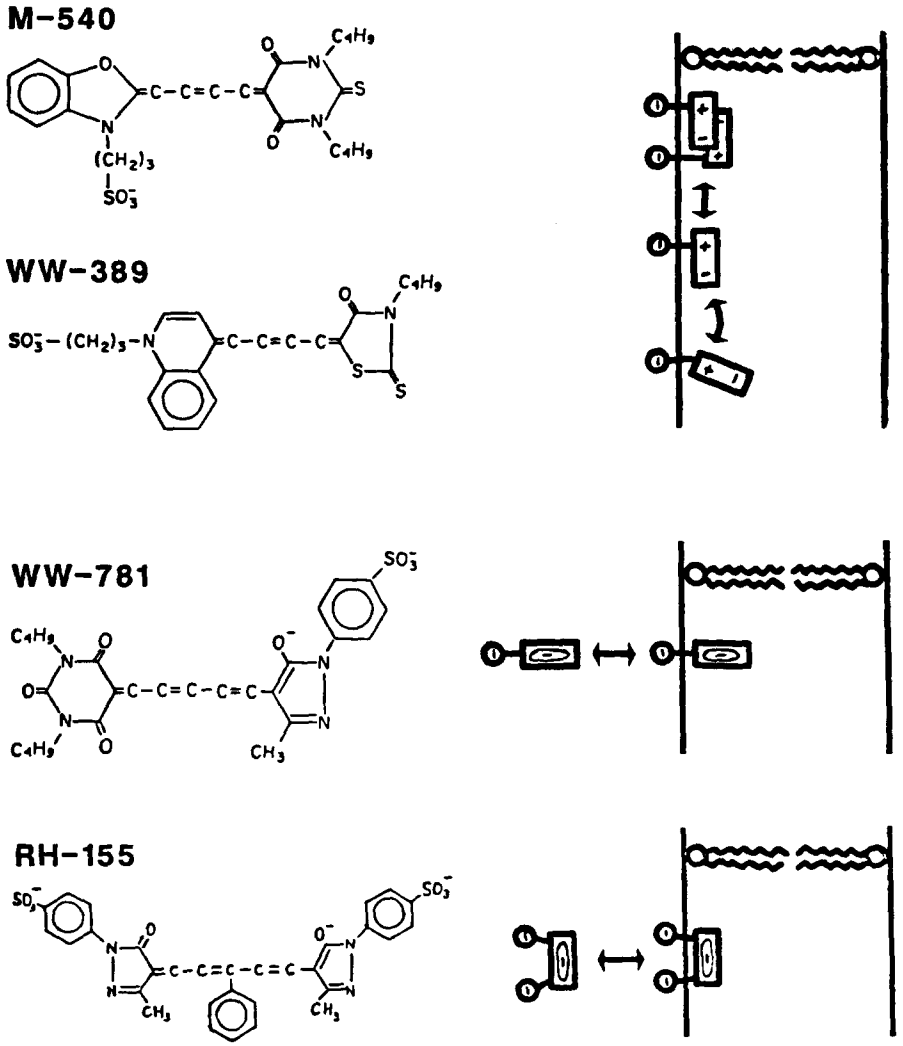

FIGURE 10. Dye structures and proposed mechanisms of action. The chromophores of the merocyanine dyes, Merocyanine-540 (M-540) and WW-389, are dipolar and are proposed to sense membrane potential by a rotation-dimer mechanism. The chromophores of the oxonol dyes, WW-781 and RH-155, have a delocalized negative charge (denoted by the oval surrounding the minus sign) and are proposed to sense potential by a rapid ON-OFF mechanism.

WW-781 was tested because it gives a large potential-dependent absorbance change in voltage-clamped squid axons (Gupta et al., 1981) and because it is the most well characterized of the oxonol dyes (George et al., 1988*a*,*b*). Like M-540, it is an amphipathic molecule with a fixed negative charge that serves as an anchor in the aqueous phase, and a hydrophobic chromophore with delocalized negative charge that penetrates a short distance into the bilayer. The center of charge of the chromophore is estimated to lie ~10 Å from the membrane surface (George et al.,

1988*b*). This molecule is thought to lie colinear with the membrane lipids and does not undergo potential-dependent rotation as with the merocyanine dyes. Instead, the potential-dependent response of oxonol dyes is attributed to an "ON-OFF" mechanism involving the rapid redistribution of dye between membrane binding sites and the aqueous phase (Waggoner, 1979). The results with this dye (not shown) were similar to those described for the merocyanine dyes. A nonlinear absorbance change appeared at depolarizing potentials positive to ~ -50 mV; in one fiber, the maximum increase of the steady-state amplitude was 40% larger than the paired hyperpolarizing amplitude (640 nm).

Finally, these experiments were repeated with the oxonol dye RH-155, which gives a large potential-dependent absorbance change in nerve membranes (Grinvald

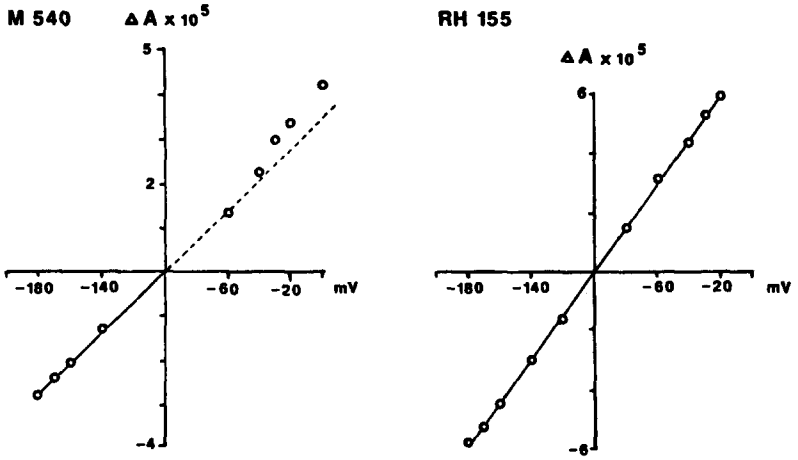

FIGURE 11. Steady-state T-system absorbance changes (O) vs. command potential (millivolts) obtained with two additional dyes, merocyanine-540 (at 570 nm) and RH-155 (at 700 nm). The steady-state absorbance change was measured at 30 ms as described for Fig. 1. For M-540, the solid line was fitted through the hyperpolarizing data points (fitted slope, 3.40×10^{-7} $\Delta A/mV$; correlation coefficient, 0.998). The dotted line is the extrapolation of the same fitted line to positive potentials. For RH-155, the solid line was fitted through all the hyperpolarizing and depolarizing data points (fitted slope factor, 7.48×10^{-7} $\Delta A/mV$; correlation coefficient, 0.999).

et al., 1986; Lev-Ram and Grinvald, 1986). In contrast to the other dyes tested, this dye has a symmetric structure, and two fixed negative charges. Because the axis of its molecular hydrophilic/hydrophobic sidedness parallels the long axis of the molecule, it is likely that the dye will sit coplanar with the membrane surface, with the fixed charges in the aqueous phase and the chromophore projecting only a short distance into the bilayer. The mechanism of RH-155 has not been systematically studied but from its homology with the oxonol family of dyes it is reasonable to infer that a similar ON-OFF mechanism might be involved (A. S. Waggoner, personal communication). The results obtained with this dye are plotted in Fig. 11 (right plot) where it can be seen that the steady-state absorbance change is linearly related to the command potential over the entire voltage range. In experiments with five addi-

tional fibers stained with this dye, the depolarizing and hyperpolarizing data could be well fit with a single straight line, with correlation coefficients of 0.998–0.999.

These results with different dyes provide additional support for the hypothesis that the nonlinear optical signal reflects a membrane-related phenomenon. The finding is not dye-specific but is detected by a variety of dyes with chromophores of different molecular structure. The two properties shared by all of the dyes that report this signal are that the chromophore has a delocalized charge or dipole moment, and that the chromophore penetrates some distance into the membrane lipid phase, where its molecular dipole moment can have some component along the direction of the transmembrane electric field. These features likewise support the idea that the nonlinear optical signal reflects an effect of an electrostatic field on the dye and not, for example, a direct binding interaction between the dye and some membrane constituent. The latter would be expected to correlate with a particular dye structure.

These results also provide some information regarding the location of the proposed electrostatic potential change. The phenomenon being reported by the merocyanine dyes and the oxonol dye WW-781 is not accessible to the oxonol dye RH-155. This strongly suggests that the phenomenon giving rise to the nonlinear optical signal is not located at the extracellular membrane surface. If a change in the electrostatic surface potential of the outer membrane face occurred, it should have been sensed by all of the dyes since all of these dyes were applied from the outside, and all of them belong to classes of dyes whose binding and spectral properties are sensitive to surface potential. These results taken together suggest that the location of the proposed electrostatic potential change is either within the bilayer or at the inner surface of the T-system membrane, perhaps at the triadic junctions that cover over 80% of the T-system area and bring it into close apposition with the sarcoplasmic reticulum.

DISCUSSION

When the T-system electrical behavior was examined using voltage-sensing dyes under presumably linear recording conditions, an unexpected nonlinearity in the optical signal was found. We first considered whether this nonlinear absorbance change might reflect voltage inhomogeneities in the T-system caused by residual unblocked ionic currents. The results suggest, in fact, that voltage-clamp control of the T-system is good under these conditions, as evidenced by the large space constant and lack of significant residual ionic currents of any kind, whether caused by passive, active or agonist activated conductances. We conclude that we do not detect any ionic currents of the magnitude required to produce the changes in T-system transmembrane potential that we detect optically, and are therefore forced to consider alternative mechanisms by which the T-system potential might change without detectable ionic current.

The most likely interpretation of the extra absorbance signal is that it reflects some local electrostatic potential change in the T-system. Such potentials would not extend beyond molecular distances of the membrane, and would not be controlled by the voltage clamp, which responds only to the potential of the bulk solution.

Moreover, a response to both transmembrane and electrostatic potential is necessarily expected for any charged or dipolar molecule in the membrane and is consistent with the mechanism of the potential-dependent response of merocyanine dyes. A large body of data indicates that most potentiometric dyes are sensitive to electrostatic potentials (Aiuchi and Kobatake, 1979; Russell et al., 1979; Krasne, 1980; Beeler et al., 1981). In particular, the spectral properties of merocyanine dyes in artificial bilayers were found to be sensitive to both surface potential and transmembrane potential (Krasne, 1980, 1983). Similarly, when put in skeletal muscle microsomes in the absence of any diffusion potential, merocyanine dyes produced spectral changes in response to induced changes in surface potential (Russell et al., 1979; Beeler et al., 1981).

Surface potentials produced by fixed charges at the membrane surface are the most well-characterized membrane electrostatic phenomena (McLaughlin, 1977). Changes in surface potential alter dye spectral properties by changing the amount of dye bound to the membrane, and/or by changing the effective transmembrane field sensed by a dipolar chromophore. An effect of an external surface potential change on dye binding cannot explain our results because all of the dyes tested bind from the outside. If a transient change in surface potential occurred at the outer membrane surface, the spectral response of all of the merocyanine and oxonol dyes should have been affected (Russell et al., 1979; Beeler et al., 1981; Krasne, 1983). On the other hand, if a transient change in surface potential occurred at the inner membrane surface, it would be expected to alter the net transmembrane field and reorient the dye molecule in a manner analogous to the effect of surface potentials on the gating subunits of ion channels (Frankenhaeuser and Hodgkin, 1957).

Our nonlinear optical signal is in the direction of extra depolarization. One way this might occur is if the inner surface potential became more positive. In general, this could occur via the loss of negative charges, the addition of positive charges, or an increased screening by cations in the adjacent solution. For example, depolarization might transiently change the concentration of a charged species bound peripherally to membrane lipids or proteins, induce the dissociation of a charged protein subunit, or move a charged membrane constituent into or out of the peripheral region within a Debye length of the bilayer.

This interpretation is summarized in the cartoon shown in Fig. 12 *A*. In this example, we assume a constant transmembrane electric field (Goldman, 1943). A positive change in the surface potential of the inner membrane leaflet would result in a more positive net transmembrane potential difference (V_m). V_m, or some fraction of V_m, is the true potential gradient to which both the dye and any membrane gating charges respond. In contrast, the voltage clamp measures and controls only the potential of the bulk solution (ΔV). It should also be noted that the mechanism postulated here would introduce positive feedback on the movement of any intramembrane gating charges, i.e., when the membrane is depolarized, the proposed local surface potential change is in a direction to cause V_m to become more positive, thereby increasing the amount of charge moved.

The model outlined in Fig. 12 *A* is the simplest proposal consistent with the data. However, it is also possible that the postulated electrostatic potential change may be within the membrane interior. For example, the movement of a charged or dipolar

protein might produce a transient change in a dipole or boundary potential within the bilayer (McLaughlin, 1977). In the previous example, both the dye and intramembrane charges were considered to respond passively to a change in an external field. In Fig. 12 *B*, we consider the possibility that the movement of intramembrane charges might itself alter the internal potential profile of the bilayer. In this case, the

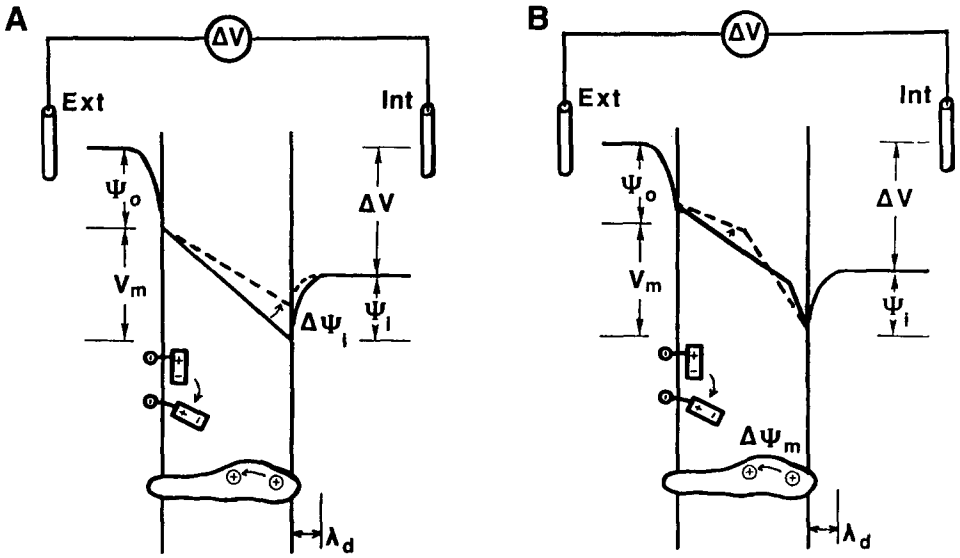

FIGURE 12. (*A*) Model of the proposed mechanism of the nonlinear absorbance signal. A local electrostatic potential change ($\Delta\psi_i$) is postulated to occur at the junctional face surface of the T-system membrane. This in turn alters the net transmembrane potential difference (V_m), which the dye and also any intramembrane charges (here symbolized on a membrane protein) experience. V_m is the sum of the applied potential difference (ΔV) and the difference between the internal and external surface potentials, $\psi_i - \psi_o$, where ψ_o and ψ_i are the local electrostatic surface potentials of the outer and inner membrane surface, respectively. The local electric field is transparent to the clamp electrodes that sense only the potential of the bulk solutions (*Ext* and *Int*). Local fields contributed by surface potentials fall off within a Debye length (λ_d) of the membrane-solution interface. (*B*) Alternative mechanism of the nonlinear absorbance change. In this case, an electrostatic potential change within the membrane interior, $\Delta\psi_m$, is itself the source of the increased local potential gradient experienced by the dye. The constant field assumption is abandoned and the intramembrane potential profile varies with distance across the bilayer. The intramembrane charges are assumed to lie in a homogeneous sheet of sufficient density so as to alter the intramembrane potential profile.

electrostatic potential gradient would not be constant across the bilayer. The relevant parameter with respect to the dye rotation is the potential gradient over the distances spanned by the dipole moment of the dye. If this becomes more positive in the outer membrane regions where the dye partitions, the dye would respond with an absorbance increase that would be indistinguishable from that produced by a change in the internal surface potential. An intramembrane electrostatic potential

change would likewise be transparent to the voltage clamp. For this mechanism to occur would probably require that the moving charges have a sufficient density so as to behave as a uniform sheet of charge, or that the dye be in high concentration near discreet moving charges so as to experience some of the dipole field in regions lateral to the protein.

Although our data itself cannot disprove this alternate possibility regarding the location of the charges generating the extra potential change, we think that an inner surface potential change (Fig. 12 *A*) is the more likely mechanism of the extra depolarization reported by the dye. Dye signals related to the gating of channel conductances have never been detected, even though early investigators in the field were specifically looking for such signals (Davila et al., 1974). Moreover, in squid axons which have a well voltage-clamped membrane, dye WW-375 gives a linear response to membrane potential over voltage regions where significant sodium gating occurs (Ross et al., 1977). This suggests either that intramembrane potential changes related to gating are small, or that they occur over membrane regions distant from the dye. Squid gating charges are in a comparable density to muscle charge movement and may share homologous gating regions with the dihydropyridine-sensitive calcium channel which is proposed to cause charge movement (Rios and Brum, 1987; Tanabe et al., 1987).

Our experiments cannot specify the physical identity of the underlying charges. However, we can exclude the possibility that the extra absorbance signal reflects a transient change in the screening of the internal surface potential by calcium ions during calcium release. Experimental tests of the Gouy-Chapman theory applied to membranes indicate that, at physiological salt concentrations, changes in calcium concentration of the magnitude that occur during calcium release (10^{-7} to 10^{-6} μM) are not expected to produce a large change in surface potential (McLaughlin et al., 1971); moreover, when we blocked calcium release with 200 μm Ruthenium Red applied to the end pool solution, the nonlinear optical signal remained (Jong, D.-S., and J. A. Heiny, unpublished results). This result suggests that transient changes in the calcium concentration of the junctional space during calcium release do not significantly alter the surface potential of the T-system membrane. It also indicates that our voltage-dependent light signal is not a consequence of calcium release.

Finally, we should point out that we cannot exclude the possibility that the extra absorbance change might result from a direct interaction of the dye with some membrane constituent rather than via an effect of an electric field on the dye. For example, if the dye binds to a membrane protein, a transient change in protein conformation might alter the dye position and spectra. Under some conditions, certain styrol and cyanine dyes are reported to give optical responses that depend on protein conformation (Ludi et al., 1983; Klodos and Forbush, 1988; Nagel et al., 1989). However, we do not think this is a likely explanation for our signal for several reasons. First, as noted, there is no correlation between dyes that sense the signal and their chromophore structure. Secondly, there does not seem to be any correlation between the amount of dye and the extra absorbance signal. Both of the above would be expected for binding phenomena. We used a hundredfold lower concentration of Merocyanine-540 than with merocyanine rhodamine dyes, but the nonlinear signal component was about the same percent increase above the linear compo-

nent in both cases. Moreover, because of the high concentrations of dye used in most of these experiments (1 mM), the density of membrane-associated dye is likely to be much greater than the density of membrane proteins. If the dye binds to some protein in a 1:1 stoichiometry, this would imply that the nonlinear absorbance change is coming from a very small fraction of the total dye molecules in the membrane, and that the absorbance change per bound dye molecule is very high.

It is difficult to measure directly the dye concentration in the membrane of an intact cell, but we can estimate a lower boundary using the Gouy equation and the measured shift of the outer surface potential produced by this concentration of dye. For example, a 0.5 mg/ml (1 mM) concentration of dye in the external solution, introduced a 10-mV negative shift of the charge-voltage curve. Assuming one negative charge per dye molecule and a 0.12 M bulk electrolyte concentration, a surface potential shift of -10 mV corresponds to a dye-related surface charge density of $\sim 50{,}000/\mu m^2$. If we take into account screening and binding by divalent ions in the T-system, then the actual density of membrane-associated dye would be higher. This approximation assumes that all of the added surface potential is contributed by screenable charge, i.e., that any dipole potential contributed by the hydrophobic chromophore of the dye is largely unscreenable and does not contribute to the measured surface potential (Krasne, 1983). This estimate can be compared with the density of some membrane proteins in muscle. The overall density of sodium channels in muscle is $\sim 650/\mu m^2$ and the density in the T-system is likely to be much lower; the density of voltage sensors in the T-system is estimated at $1{,}000$–$1{,}500/\mu m^2$ (cf. Almers, 1978). This suggests that our dye-protein ratio is much greater than one.

In summary, when potentiometric dyes were used to monitor the T-system voltage change under passive recording conditions, we detected an extra nonlinear optical signal that cannot be explained by voltage clamp or dye-related artifacts. The speed, stoichiometry, and lack of dependence of this signal on a particular dye structure all suggest that it arises from an electric field effect on the dye. We propose that a local electrostatic potential change occurs in the T-system upon depolarization. This phenomenon shares several features in common with charge movement and mechanical activation, suggesting that it may be associated with excitation-contraction coupling. This association will be the subject of further investigations.

The authors wish to thank Dr. Alan Waggoner for the gift of dye WW-389 and for helpful information regarding dye mechanisms. In addition, the authors thank Drs. L. Cohen, B. Forbush, and S. Krasne for helpful discussions and Dr. M. Behbehani for criticisms of the manuscript. Portions of this work were submitted by D. Jong to the University of Cincinnati in partial fulfillment of the requirements for the Ph.D. in Physics.

This work was supported by National Science Foundation grant DCB-8508305 and a research grant from the Muscular Dystrophy Association. Dr. Heiny is a recipient of an Established Investigator Award from the American Heart Association, with funds contributed in part by the American Heart Association-Ohio Affiliate.

Original version received 21 December 1988 and accepted version received 6 June 1989.

REFERENCES

Aiuchi, T., and Y. Kobatake. 1979. Electrostatic interaction between Merocyanine 540 and liposomal and mitochondrial membranes. *Journal of Membrane Biology.* 45:233–244.

Adrian, R. H., and W. Almers. 1974. Membrane capacity measurements on frog skeletal muscle in media of low ion content. *Journal of Physiology.* 237:573–605.

Adrian, R. H., W. K. Chandler, and A. L. Hodgkin. 1969. The kinetics of mechanical activation in frog muscle. *Journal of Physiology.* 204:207–230.

Adrian, R. H., W. K. Chandler, and R. F. Rakowski. 1976. Charge movement and mechanical repriming in skeletal muscle. *Journal of Physiology.* 254:361–388.

Adrian, R. H., and C. L.-H. Huang. 1984. Charge movements near the mechanical threshold in skeletal muscle of *Rana temporaria. Journal of Physiology.* 349:483–500.

Adrian, R. H., and L. D. Peachey. 1973. Reconstruction of the action potential of frog sartorius muscle. *Journal of Physiology.* 163:105–115.

Almers, W. 1978. Gating currents and charge movements in excitable membranes. *Reviews of Physiology, Biochemistry and Pharmacology.* 82:96–190.

Ashcroft, F. M., J. A. Heiny, and J. Vergara. 1985. Inward rectification in the T-system of frog skeletal muscle, studied with potentiometric dyes. *Journal of Physiology.* 359:269–291.

Beeler, T. J., R. H. Farmen, and A. Martonosi. 1981. The mechanism of voltage-sensitive dye responses on sarcoplasmic reticulum. *Journal of Membrane Biology.* 62:113–137.

Brown, K. M., and J. E. Dennis. 1972. Derivitive free analogues of the Levenberg-Marquardt and Gauss algorithms for non-linear square approximations. *Numerische Mathematik.* 18:289–297.

Chandler, W. K., R. F. Rakowski, and M. F. Schneider. 1976*a*. A non-linear voltage-dependent charge movement in frog skeletal muscle. *Journal of Physiology.* 254:243–283.

Chandler, W. K., R. F. Rakowski, and M. F. Schneider. 1976*b*. Effects of glycerol treatment and maintained depolarization on charge movement in skeletal muscle. *Journal of Physiology.* 254:285–316.

Cohen, L. B., and B. M. Salzberg. 1978. Optical measurements of membrane potential. *Reviews of Physiology, Biochemistry and Pharmacology.* 83:35–88.

Cohen, L. B., B. M. Salzberg, H. V. Davila, W. N. Ross, D. Landowne, A. S. Waggoner, and C. H. Wang. 1974. Changes in axon fluorescence during activity: molecular probes of membrane potential. *Journal of Membrane Biology.* 19:1–36.

Davila, H. V., L. B. Cohen, B. M. Salzberg, and B. B. Shrivastav. 1974. Changes in ANS and TNS fluorescence in giant axons from *Loligo. Journal of Membrane Biology.* 15:29–46.

Dragsten, P. R., and W. W. Webb. 1978. Mechanism of the membrane potential sensitivity of the fluorescent membrane probe Merocyanine 540. *Biochemistry.* 17:5228–5240.

Dulhunty, A., and P. Gage. 1973. Electrical properties of toad sartorius muscle fibres in summer and winter. *Journal of Physiology.* 230:619–641.

Falk, G. 1968. Predicted delays in the activation of the contractile system. *Biophysical Journal.* 8:608–625.

Frankenhaeuser, B., and A. L. Hodgkin. 1957. The action of calcium on the electrical properties of squid axons. *Journal of Physiology.* 137:218–244.

George, E. B., P. Nyirjesy, M. Basson, L. A. Ernst, P. R. Pratap, J. C. Freedman, and A. S. Waggoner. 1988*a*. Impermeant potential-sensitive oxonol dyes: I. Evidence for an "on-off" mechanism. *Journal of Membrane Biology.* 103:245–253.

George, E. B., P. Nyirjesy, P. R. Pratap, J. C. Freedman, and A. S. Waggoner. 1988*b*. Impermeant potential-sensitive oxonol dyes: III. The dependence of the absorption signal on membrane potential. *Journal of Membrane Biology.* 105:55–64.

Godt, R. E., and B. D. Lindley. 1982. Influence of temperature upon contractile activation and isometric force production in mechanically skinned muscle fibers of the frog. *Journal of General Physiology.* 80:279–297.

Godt, R. E., and D. W. Maughan. 1988. On the composition of the cytosol of relaxed skeletal muscle of the frog. *American Journal of Physiology.* 254:C591–C604.

Goldman, D. E. 1943. Potential, impedance, and rectification in membranes. *Journal of General Physiology.* 27:37–60.

Grinvald, A., A. Manker, and M. Segal. 1986. Visualization of the spread of electrical activity in rat hippocampal slices by voltage-sensitive optical probes. *Journal of Physiology.* 333:269–291.

Gupta, R. R., B. M. Salzberg, A. Grinvald, L. B. Cohen, R. Kamino, S. Lesher, M. B. Boyle, A. S. Waggoner, and C. H. Wang. 1981. Improvements in optical methods for measuring rapid changes in membrane potential. *Journal of Membrane Biology.* 58:123–137.

Heiny, J. A., and D. Jong. 1989. Non-linear T-system voltage changes detected optically under "linear" charge movement recording conditions. *Biophysical Journal.* 55:238*a*. (Abstr.)

Heiny, J. A., and J. Vergara. 1982. Optical signals from surface and T-system membranes in skeletal muscle fibers. Experiments with the potentiometric dye NK2367. *Journal of General Physiology.* 80:203–230.

Heiny, J. A., and J. Vergara. 1984. Dichroic behavior of the absorbance signals from dyes NK2367 and WW375 in skeletal muscle fibers. *Journal of General Physiology.* 84:805–837.

Hille, B., and D. T. Campbell. 1976. An improved vaseline-gap voltage-clamp for skeletal muscle fibers. *Journal of General Physiology.* 67:265–293.

Hodgkin, A. L., and P. Horowicz. 1960. Potassium contractures in single muscle fibers. *Journal of Physiology.* 153:386–403.

Horowicz, P., and M. F. Schneider. 1981. Membrane charge movement in contracting and non-contracting skeletal muscle fibres. *Journal of Physiology.* 314:565–593.

Irving, M., J. Maylie, N. L. Sizto, and W. K. Chandler. 1987. Intrinsic optical and passive electrical properties of cut frog twitch fibers. *Journal of General Physiology.* 89:1–40.

Jong, D., and J. A. Heiny. 1988. T-system voltage changes and charge movement in skeletal muscle. *FASEB Journal.* 2:A334. (Abstr.)

Jong, D., and J. A. Heiny. 1989. Origin of the non-linear T-system potential changes: a possible association with E-C coupling? *Biophysical Journal.* 55:238*a*. (Abstr.)

Klodos, I., and B. Forbush. 1988. Rapid conformational changes of the Na/K pump revealed by a fluorescent dye, RH-160. *Journal of General Physiology.* 92:46*a*. (Abstr.)

Krasne, S. 1980. Interactions of voltage-sensing dyes with membranes. II. Spectrophotometric and electrical correlates of cyanine-dye adsorption to membranes. *Biophysical Journal.* 30:441–462.

Krasne, S. 1983. Interactions of voltage-sensing dyes with membranes. III. Electrical properties induced by Merocyanine 540. *Biophysical Journal.* 44:305–314.

Lev-Ram, V., and A. Grinvald. 1986. Ca^{2+}- and K^{+}-dependent communication between central nervous system myelinated axons and oligodendrocytes revealed by voltage-sensitive dyes. *Proceedings of the National Academy of Sciences.* 83:6651–6655.

Ludi, H., H. Oetliker, U. Brodbeck, P. Ott, B. Schwendimann, and B. Fulpius. 1983. Reconstitution of pure acetylcholine receptor in phospholipid vesicles and comparison with receptor-rich membranes by the use of a potentiometric dye. *Journal of Membrane Biology.* 74:75–84.

Martell, A. E., and R. M. Smith. 1974. Critical stability constants, Vol. 1: amino acids. Plenum Publishing Co., New York. 27 and 269–270.

McLaughlin, S. G. A. 1977. Electrostatic potentials at membrane-solution interfaces. *Current Topics in Membranes and Transport.* 9:71–144.

McLaughlin, S. G. A., G. Szabo, and G. Eisenman. 1971. Divalent ions and the surface potential of charged phospholipid membranes. *Journal of General Physiology.* 58:667–687.

Nagel, G., C. Slayman, and I. Klodos. 1989. Fluorescence probing of a major conformation change in the plasma membrane H-ATPase of Neurospora. *Biophysical Journal.* 55:338*a* (Abstr.)

Nakajima, S., and A. Gilai. 1980. Action potentials of isolated single muscle fibers recorded by potential-sensitive dyes. *Journal of General Physiology.* 76:729–750.

Neville, M. C., and S. White. 1979. Extracellular space of frog skeletal muscle in vivo and in vitro: relation to proton magnetic resonance relaxation times. *Journal of Physiology.* 288:71–83.

Rios, E., and G. Brum. 1987. Involvement of dihydropyridine receptors in excitation-contraction coupling in skeletal muscle. *Nature.* 325:717–720.

Ross, W. N., B. M. Salzberg, L. B. Cohen, A. Grinvald, H. V. Davila, A. S. Waggoner, and C. H. Wang. 1977. Changes in absorption, fluorescence, dichroism and birefringence in stained giant axons: optical measurement of membrane potential. *Journal of Membrane Biology.* 33:141–183.

Russell, J. T., T. Beeler, and A. Martonosi. 1979. Optical probe responses on sarcoplasmic reticulum; merocyanine and oxonol dyes. *Journal of Biological Chemistry.* 254:2047–2052.

Schneider, M. F., and W. K. Chandler. 1973. Voltage-dependent charge movement in skeletal muscle: a possible step in excitation-contraction coupling. *Nature.* 242:244–246.

Smith, R. M., and A. E. Martell. 1976. Critical stability constants, Vol. 4: inorganic complexes. Plenum Publishing Co., New York. 79–82.

Tanabe, T., H. Takeshima, A. Mikami, V. Flockerzi, H. Takahashi, K. Kangawa, M. Kojima, H. Matsuo, T. Hirose, and S. Numa. 1987. Primary structure of the receptor for calcium channel blockers from skeletal muscle. *Nature.* 328:313–318.

Vergara, J., and F. Bezanilla. 1981. Optical studies of E-C coupling with potentiometric dyes. *In* The Regulation of Muscle Contraction: Excitation-Contraction Coupling. A. Grinnell and M. Brazier, editors. Academic Press, Inc., New York. 67–77.

Waggoner, A. S. 1979. Dye indicators of membrane potential. *Annual Reviews of Biophysics and Bioengineering.* 8:47–68.

Waggoner, A., and A. Grinvald. 1977. Mechanisms of rapid optical changes of potential sensitive dyes. *Annals of the New York Academy of Sciences.* 303:217–241.

Warashina, A., and I. Tasaki. 1975. Evidence for rotation of dye molecules in membrane macromolecules associated with nerve excitation. *Proceedings of the Japanese Academy.* 51:610–615.

Wolf, B. E., and A. S. Waggoner. 1986. Optical studies of the mechanism of membrane potential sensitivity of Merocyanine 540. *In* Optical Methods in Cell Physiology. P. DeWeer and B. M. Salzberg, editors. John Wiley and Sons, New York. 101–113.